Constructing an Unprecedented $\{Mn^{II}_{38}\}$ Matryoshka Doll with $[Mn_{18}(CO_3)_9]$ Inorganic Core and Magnetocaloric Effect†

Tai-Xue Wu, Ye Tao, Qiu-Ju He, Hai-Ye Li,* He-Dong Bian, Fu-Ping Huang*

Table of the content

1. General Materials and Methods
2. X-ray Structure Determination
3. Synthesis of **1**.
4. Table S1. Crystal data and structure refinement parameters for **1**.
5. Table S2. Selected bond lengths (Å) and angles (°) for **1**.
6. Table S3. Bond Valence Sum (BVS)^{a}, Calculations for Mn Atoms in **1**.
7. Fig. S1. A photo of the crystals of **1** taken under the microscope showing their regular shape color and size.
8. Fig. S2. The FTIR spectra of **1** recorded in KBr palates.
9. Fig. S3. The coordination environments of Mn^{II} ions of **1**.
10. Fig. S4. The coordination mode of the ligand.
11. Fig. S5. The 3D framework of **1**.
12. Fig. S6. The structure of the anion coordination cage within complex **1** composed of three groups of ligands.
13. Fig.S7. (Left eight disorder carbonate anions on the facial of the octahedron coordinate with six Mn to form a highly symmetrical cage in which one carbonate anion resides; (Right the structure and size of the coordination space of carbonate anion is provided by the space-filling plots.
14. Fig. S8. The XPS full-survey scan spectra of complex **1**.
15. Fig. S9. The Mn 3s XPS spectra of **1**.
16. Fig. S10. A Plot of $\chi_M T$ vs T for **1**.
17. Fig. S11. The χ_m^{-1}-T plot for **1**.
18. Fig. S12. Field dependence of the magnetization at 2.0 K of **1**.
19. Fig. S13. Out-of-phase ac χ'_M and χ''_M *vs* T at the indicated frequencies for **1**.
20. Fig. S14. The plot of M-H for **1** in the field rang of 0-50 kOe at 2-6 K.

21. References.

---

a State Key Laboratory for the Chemistry and Molecular Engineering of Medicinal Resources, School of Chemistry and Pharmacy, Guangxi Normal University, Guilin 541004, P. R. China. Fax: +86-773-2120958; E-mail: lihaiye2010@163.com (H. Y. Li); huangfp2010@163.com (F. P. Huang)

General Materials and Methods

All reagents were used as received without further purification. IR spectra were recorded in the range of 4000-400 cm^{-1} on a Perkin-Elmer Spectrum One FT/IR spectrometer using a KBr pellet. Elemental microanalyses for C, H, and N were carried out on a Model 2400 II, Perkin-Elmer elemental analyzer. X-ray photoelectron spectroscopy (XPS) measurement was performed with a Kratos Axis Ultra DLD spectrometer. Magnetic susceptibility measurements were performed in the temperature range of 300-2 K using a Quantum Design MPMS SQUIDXL-5 magnetometer equipped with a 7 T magnetic field. The diamagnetic correction for the complex was estimated using Pascal's constants, and magnetic data were corrected for diamagnetic contributions of the sample holder.

X-ray Structure Determination

Single crystals of **1** was chosen under an optical microscope and mounted on a CryoLoop for data collection. All reflection data were collected on an Rigaku Oxford Diffraction diffractometer (Cu, λ= 1.54184 Å) at room temperature. The data integration and reduction were processed using CrysAlisPro software and the structures were solved by direct methods using ShelXS and refined using a full-matrix least-squares technique within ShelXL 2014 and OLEX-2 Program.[S1-S3] All non-hydrogen atoms were refined anisotropically until convergence is reached. Hydrogen atoms attached to the organic moieties present in all compounds are either located from the difference Fourier map or stereochemically fixed. Summary of crystallographic data and details of data collection for **1** is given in Table S1. Selected bond lengths and angles for **1** is collected in Table S2. Crystallographic data for the structural analyses has been deposited at the Cambridge Crystallo-graphic Data Centre (CCDC reference numbers: (2032515)

Synthesis of $[(CH_3)_2NH_2]_6[Mn_{38}(\mu_6\text{-}CO_3)_9(\mu_2\text{-}O)_6Cl_{24}(bmpbt)_{12}(H_2bmpbt)_6]\cdot[MnCl_4]_2$(1).

1 was prepared under solvothermal conditions. A mixture of $MnCl_2\cdot 4H_2O$ (49.5 mg, 0.5 mmol), H_2bmpbt (31.8mg, 0.1 mmol), Na_2CO_3(10.6mg, 0.05mmol), DMF (7 mL), CP（acetone）(7mL) and triethylamine (50uL) was placed in a 25 mL Teflon-lined stainless steel vessel and heated at 180 °C for 48 h and then cooled to room temperature at a rate of 5 °C, and finally the pale yellow rice grain shaped crystal of **1** were obtained by washing it with distilled water, then picking out after being dried in air. Yield: 20 % (base on Mn (II)). Elemental analysis (%): Calcd: C, 37.28; H, 2.80; N, 21.12. Found: C, 36.62; H, 2.33; N, 20.83. IR (KBr, cm^{-1}): 3432 (vs), 2953 (w) ,1613m, 1466m, 1437w, 1376m, 1294m, 1149m,1039w, 1005w, 853w, 759w, 568w, 498w.

Table S1. Crystallographic data and structure refinement parameters for 1.

Complex	**1**
Empirical formula	$C_{297}H_{228}Cl_{24}Mn_{38}N_{144}O_{33}\cdot 2(MnCl_4)\cdot 6(C_2H_8N)$
Formula weight	9950.78

Crystal system	Trigonal
Space group	*R*-3
a (Å)	25.0072 (12) Å
b (Å)	25.0072(12)
c (Å)	55.114(2)
γ (°)	120.00
V/(Å^3)	29849(3)
Z	3
*D*c(Mg cm^{-3})	1.661
F(000)	14964.0
θ range for data collection (°)	3.5–65.2°
Reflections collected/unique	42960/11723 [R_{int} = 0.123]
Goodness-of-fit on F^2	1.027
Final *R* indices [$I > 2\sigma(I)$]	R_1 = 0.1009; ωR_2 = 0.2738
R indices (all data)	R_1 = 0.1854; ωR_2 = 0.3433

Table S2. Selected bond lengths (Å) and angles (º) for **1**

Mn1—N3	2.177 (9)	Mn4—N1i	2.284 (10)
Mn1—N7	2.178 (8)	Mn4—N4i	2.217 (9)
Mn1—N15	2.170 (9)	Mn4—N6	2.210 (9)
Mn1—O2'	2.237 (14)	Mn4—N8	2.309 (10)
Mn1—O3'i	2.246 (15)	Mn4—N17	2.369 (11)
Mn1—O1'	2.103 (14)	Mn4—N18	2.181 (8)
Mn1—O2i	2.134 (15)	Mn5—N23	2.163 (8)
Mn2—O6	2.274 (18)	Mn5—N23ii	2.162 (8)
Mn2—N12	2.302 (9)	Mn5—N23iii	2.163 (8)
Mn2—N14	2.369 (10)	Mn5—N24	2.332 (9)
Mn2—O1	2.207 (13)	Mn5—N24ii	2.332 (9)
Mn2—O2'i	2.245 (13)	Mn5—N24iii	2.332 (9)

Mn2—O3'ii	2.225 (15)	Mn6—Cl1	2.466 (6)
Mn2—O4	2.297 (19)	Mn6—Cl2	2.249 (7)
Mn2—O1'	2.220 (13)	Mn6—O5	2.085 (11)
Mn2—O2i	2.182 (14)	Mn6—N13	2.264 (10)
Mn2—O3ii	2.209 (15)	Mn6—N16	2.338 (12)
Mn2—O4'	2.19 (2)	Mn7—Cl3	2.384 (5)
Mn3—N11	2.162 (10)	Mn7—Cl4	2.197 (14)
Mn3—N20i	2.188 (8)	Mn7—O5	2.079 (9)
Mn3—N22i	2.223 (8)	Mn7—N9	2.347 (11)
Mn3—O1ii	2.266 (14)	Mn7—N10	2.268 (9)
Mn3—O4	2.082 (18)	Mn8—Cl5	2.370(14)
Mn3—O3ii	2.195 (14)	Mn8—Cl6	2.393(7)
Mn3—O4'ii	2.279 (17)	Mn8—Cl6iv	2.392(7)
		Mn8—Cl5v	2.392(7)
N3—Mn1—N7	75.1 (3)	N20i—Mn3—O1ii	79.6 (4)
N3—Mn1—O2'	81.8 (4)	N20i—Mn3—O4'ii	116.4 (6)
N3—Mn1—O3'i	121.6 (4)	N22i—Mn3—O1ii	120.3 (4)
N7—Mn1—O2'	120.7 (4)	N22i—Mn3—O4'ii	80.2 (5)
N7—Mn1—O3'i	81.0 (4)	O4—Mn3—N11	88.0 (6)
N15—Mn1—N3	105.4 (3)	O4—Mn3—N20i	162.3 (6)
N15—Mn1—N7	105.8 (3)	O3ii—Mn3—N22i	162.3 (4)
N15—Mn1—O2'	132.9 (4)	O3ii—Mn3—O4'ii	84.4 (6)
N15—Mn1—O3'i	132.4 (5)	N1i—Mn4—N8	89.2 (4)
O2'—Mn1—O3'i	66.4 (5)	N1i—Mn4—N17	89.8 (4)
O1'—Mn1—N3	104.9 (4)	N4i—Mn4—N1i	73.3 (4)
O1'—Mn1—N7	162.9 (4)	N4i—Mn4—N8	162.5 (4)
O1'—Mn1—N15	90.8 (4)	N4i—Mn4—N17	90.2 (4)
O1'—Mn1—O2i	68.8 (5)	N6—Mn4—N1i	89.9 (4)

O2i—Mn1—N3	165.4 (4)	N6—Mn4—N4i	105.5 (3)
O2i—Mn1—N7	106.9 (4)	N6—Mn4—N8	73.7 (4)
O2i—Mn1—N15	88.2 (4)	N6—Mn4—N17	163.5 (4)
O6—Mn2—N12	145.9 (10)	N8—Mn4—N17	89.8 (4)
O6—Mn2—N14	146.2 (10)	N18—Mn4—N1i	162.3 (4)
O6—Mn2—O4	77.9 (10)	N18—Mn4—N4i	103.0 (3)
N12—Mn2—N14	67.8 (3)	N18—Mn4—N6	107.7 (3)
N12—Mn2—O4	73.0 (6)	N18—Mn4—N8	93.7 (3)
O1—Mn2—O6	76.5 (12)	N18—Mn4—N17	72.8 (3)
O1—Mn2—N12	118.3 (4)	N23ii—Mn5—N23iii	102.3 (3)
O1—Mn2—N14	83.9 (4)	N23ii—Mn5—N23	102.3 (3)
O1—Mn2—O2'i	109.4 (5)	N23iii—Mn5—N23	102.3 (3)
O1—Mn2—O3'ii	155.0 (5)	N23ii—Mn5—N24iii	165.1 (3)
O1—Mn2—O4	86.4 (6)	N23—Mn5—N24	74.2 (3)
O2'i—Mn2—O6	78.2 (9)	N23ii—Mn5—N24	92.6 (3)
O2'i—Mn2—N12	119.2 (4)	N23—Mn5—N24iii	92.6 (3)
O2'i—Mn2—N14	82.8 (4)	N23ii—Mn5—N24ii	74.2 (3)
O2'i—Mn2—O4	147.2 (6)	N23iii—Mn5—N24	165.1 (3)
O3'ii—Mn2—O6	78.5 (12)	N23iii—Mn5—N24ii	92.6 (3)
O3'ii—Mn2—N12	82.4 (4)	N23—Mn5—N24ii	165.1 (3)
O3'ii—Mn2—O2'i	66.6 (5)	N24iii—Mn5—N24	91.3 (3)
O3'ii—Mn2—O4	86.8 (6)	N24ii—Mn5—N24iii	91.3 (3)
O4—Mn2—N14	128.5 (5)	N24ii—Mn5—N24	91.3 (3)
O1'—Mn2—O6	77.5 (12)	Cl2—Mn6—Cl1	101.0 (3)
O1'—Mn2—N12	128.8 (4)	Cl2—Mn6—N13	110.8 (3)
O1'—Mn2—N14	73.8 (4)	Cl2—Mn6—N16	100.4 (3)

O2i—Mn2—O6	79.2 (9)	O5—Mn6—Cl1	94.0 (3)
O2i—Mn2—N12	128.4 (4)	O5—Mn6—Cl2	108.1 (3)
O2i—Mn2—N14	73.1 (4)	O5—Mn6—N13	89.7 (3)
O2i—Mn2—O1'	65.9 (5)	O5—Mn6—N16	150.2 (4)
O2i—Mn2—O3ii	108.2 (6)	N13—Mn6—Cl1	145.1 (3)
O2i—Mn2—O4'	149.8 (6)	N13—Mn6—N16	72.0 (4)
O3ii—Mn2—O6	77.0 (12)	N16—Mn6—Cl1	88.7 (3)
O3ii—Mn2—N12	75.1 (4)	Cl4—Mn7—Cl3	105.0 (4)
O3ii—Mn2—N14	129.7 (5)	Cl4—Mn7—N9	108.3 (5)
O3ii—Mn2—O1'	154.5 (5)	Cl4—Mn7—N10	91.0 (4)
O4'—Mn2—O6	77.3 (10)	O5—Mn7—Cl3	98.8 (3)
O4'—Mn2—N12	80.9 (6)	O5—Mn7—Cl4	108.3 (6)
O4'—Mn2—N14	120.1 (5)	O5—Mn7—N9	138.1 (4)
O4'—Mn2—O1'	90.6 (5)	O5—Mn7—N10	88.0 (3)
O4'—Mn2—O3ii	84.7 (6)	N9—Mn7—Cl3	90.8 (3)
N11—Mn3—N20i	109.1 (3)	N10—Mn7—Cl3	159.4 (3)
N11—Mn3—N22i	108.8 (3)	N10—Mn7—N9	71.7 (4)
N11—Mn3—O1ii	130.5 (4)	Cl5—Mn8—Cl6	110.9 (2)
N11—Mn3—O3ii	88.2 (4)	Cl5—Mn8—Cl6iv	110.9 (2)
N11—Mn3—O4'ii	134.3 (6)	Cl5—Mn8—Cl6v	110.8 (2)
N20i—Mn3—N22i	74.4 (3)	Cl6iv—Mn8—Cl6v	108.1 (3)
O4—Mn3—N22i	104.8 (6)	Cl6iv—Mn8—Cl6	108.1 (3)
O4—Mn3—O1ii	86.0 (6)	Cl6—Mn8—Cl6v	108.1 (3)
O3ii—Mn3—N20i	105.2 (4)		

Symmetry codes: (i) *x*-*y*+1/3, *x*-1/3, -*z*+2/3; (ii) -*y*+1, *x*-*y*, *z*; (iii) -*x*+*y*+1, -*x*+1, *z*; (iv) 2-*y*, 1+*x*-*y*, *z*; (v) 1+*y*-*x*, 2-*x*, *z*

Table S3. Bond Valence Sum (BVS)^{a}, Calculations for Mn Atoms in **1** [S4-S7]

Atom	**Mn(II)**	Mn(III)	Mn(IV)
Mn1	**2.262**	2.145	2.077
Mn2	**1.977**	1.849	1.802
Mn3	**2.071**	1.965	1.903
Mn4	**1.997**	1.934	1.857
Mn5	**2.095**	2.028	1.948
Mn6	**2.180**	2.147	2.086
Mn7	**2.384**	2.355	2.289
Mn8	**2.010**	2.048	1.994

a The underlined value is the one closest to the charge for which it was calculated. The oxidation state is the nearest whole number to the underlined value.

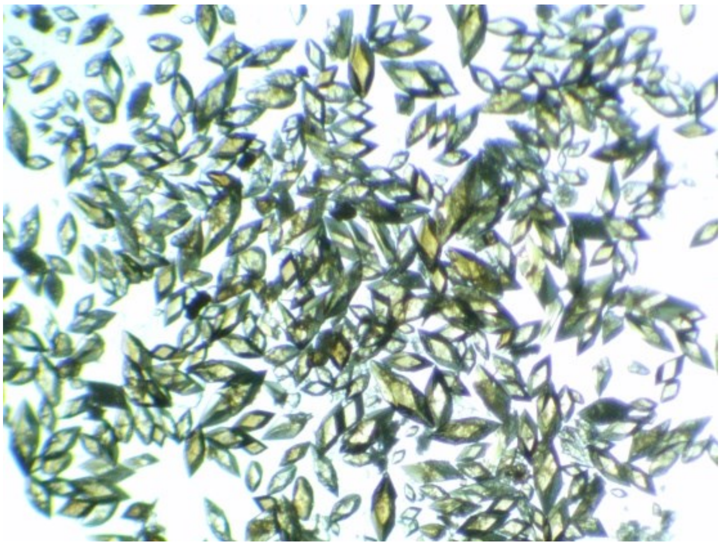

Fig. S1. A photo of the crystals of **1** taken under the microscope showing their regular shape color and size**.**

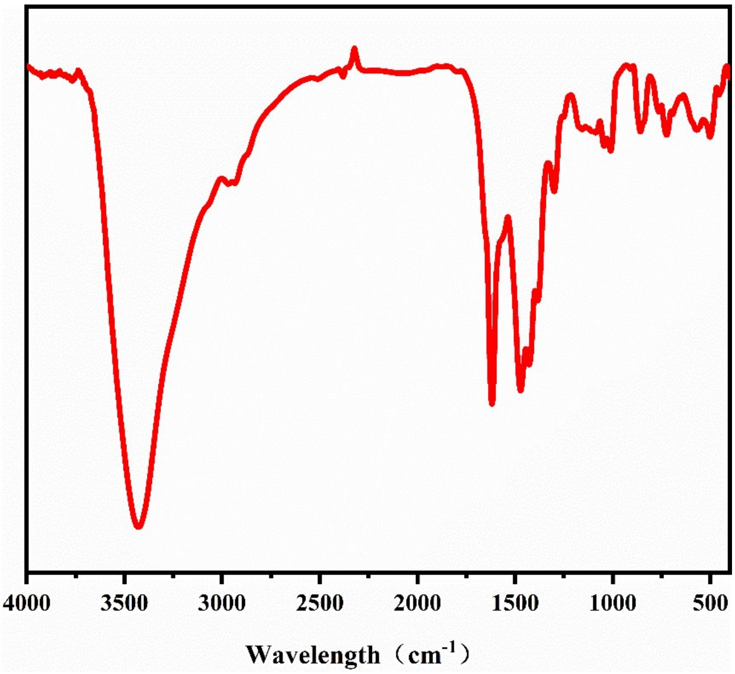

Fig. S2. The FTIR spectra of **1** recorded in KBr palates.

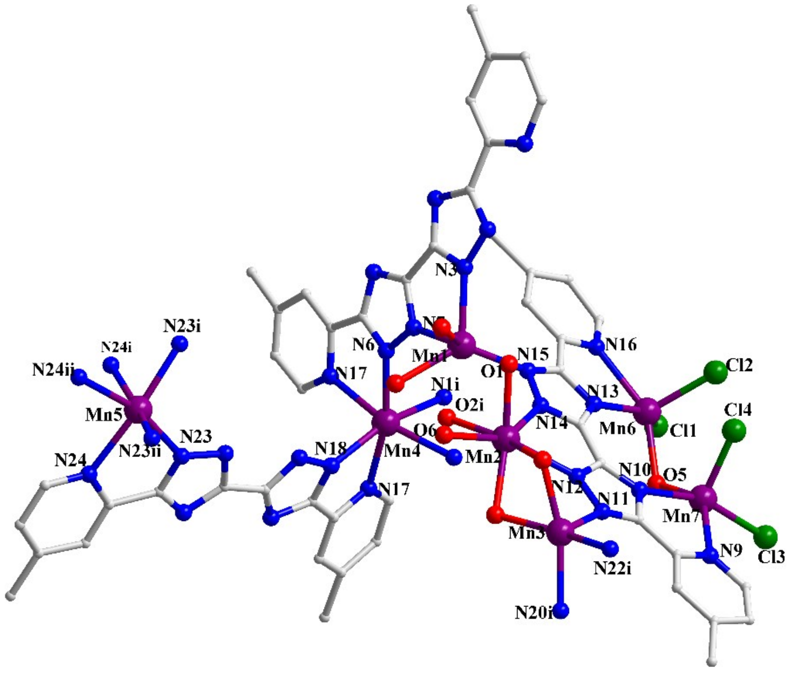

Fig. S3. The coordination environments of Mn^{II} ions of **1**.

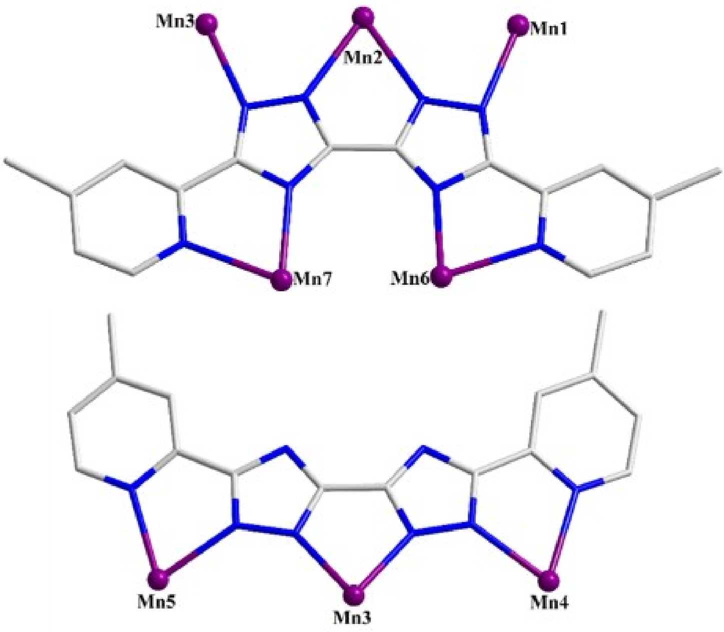

Fig. S4. The coordination mode of the ligand.

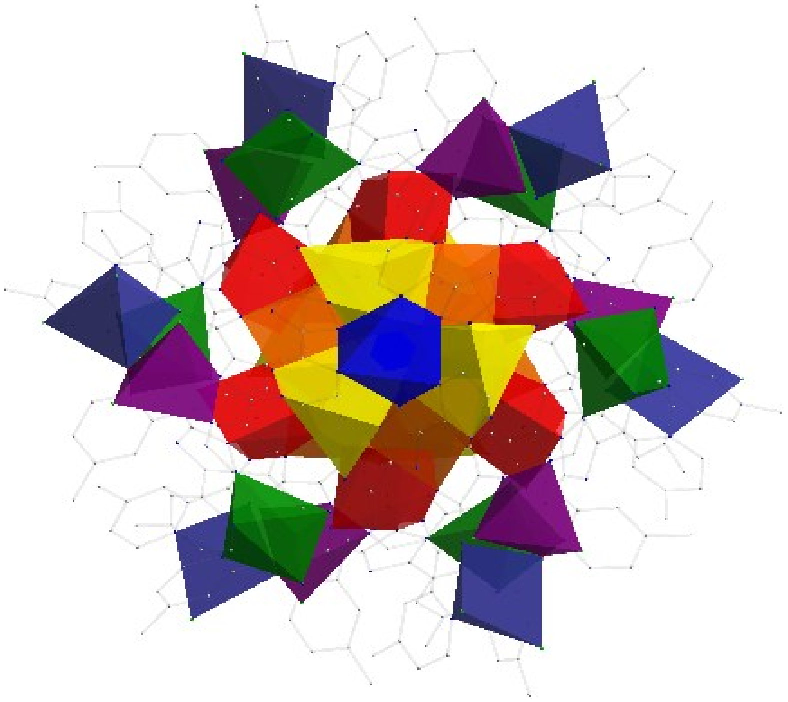

Fig. S5. The 3D framework of **1**, and the red polyhedra represent $[Mn1^{II}N_3O_2]$ units; the orange polyhedra represent $[Mn2^{II}N_2O_5]$ units; the green polyhedra represent $[Mn3^{II}N_3O_2]$ units; the blue polyhedra represent $[Mn4^{II}N_6]$ units;the indigo polyhedra represent $[Mn5^{II}N_6]$ units; the violet polyhedra represent $[Mn6^{II}N_2OCl_2]$ units; the purple polyhedra represent $[Mn7^{II}N_2OCl_2]$ units.

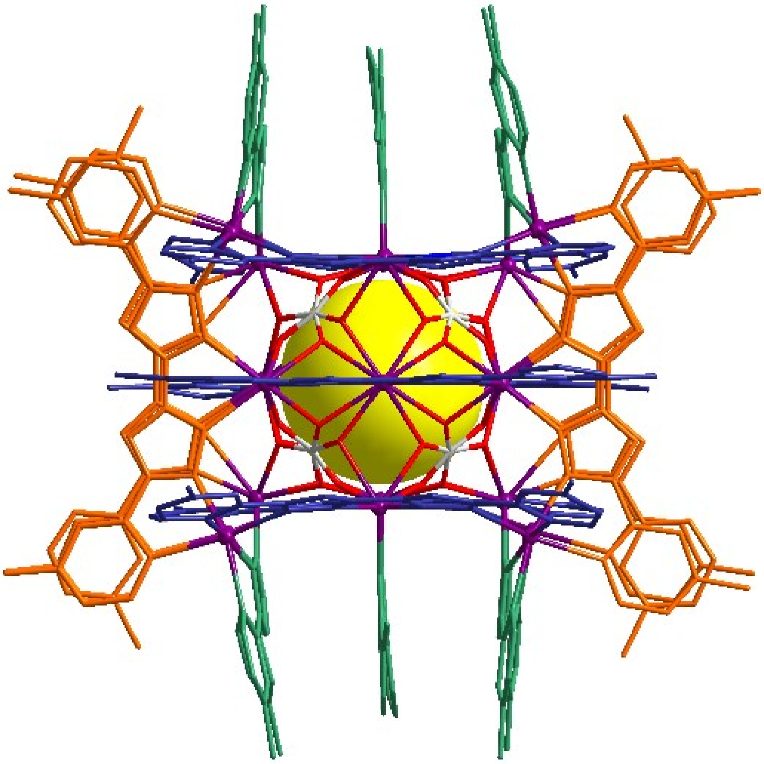

Fig. S6. The structure of the anion coordination cage within complex **1** composed of three groups of ligands. The big ball represents the carbanion anion, which resides in the inner of the anion cage and acts as the counterion of the cage.

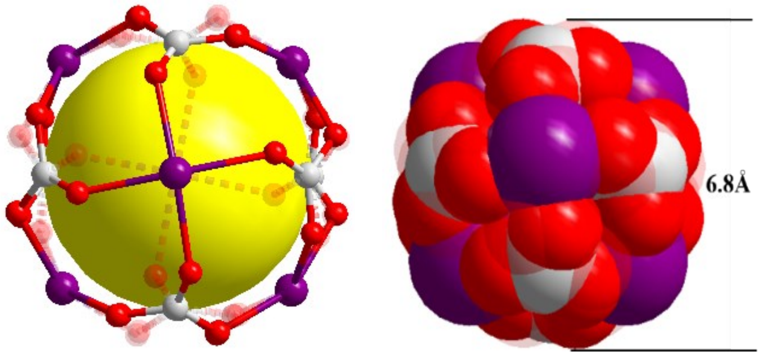

Fig.S7. (Left eight disorder carbonate anions on the facial of the octahedron coordinate with six Mn to form a highly symmetrical cage in which one carbonate anion resides; (Right the structure and size of the coordination space of carbonate anion is provided by the space-filling plots.

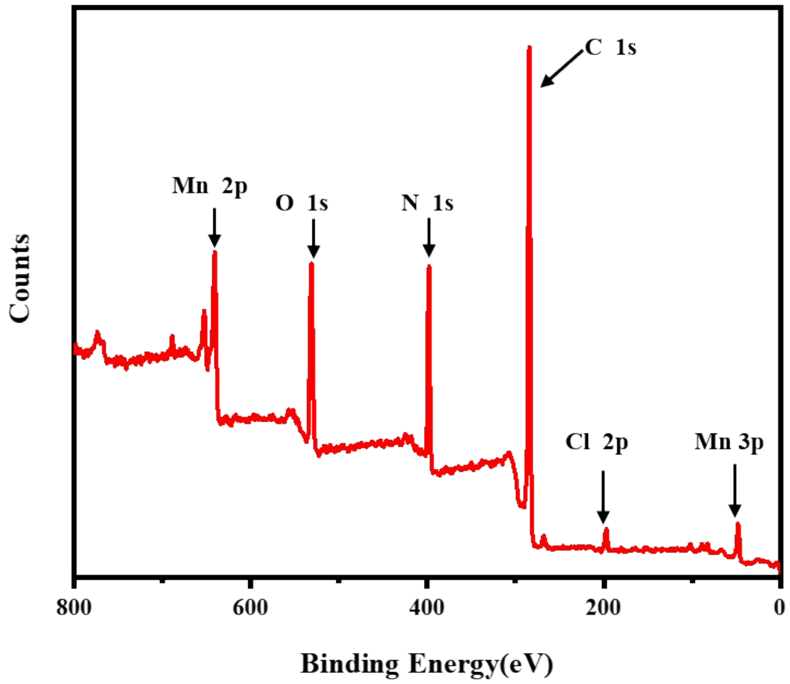

Fig. S8. The XPS full-survey scan spectra of complex **1**.

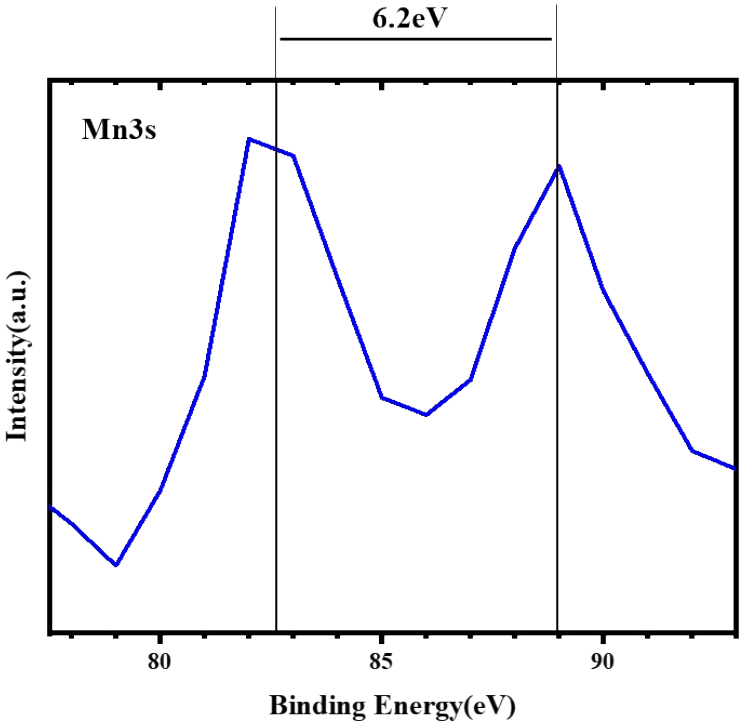

Fig. S9. The Mn 3s XPS spectra of **1**.

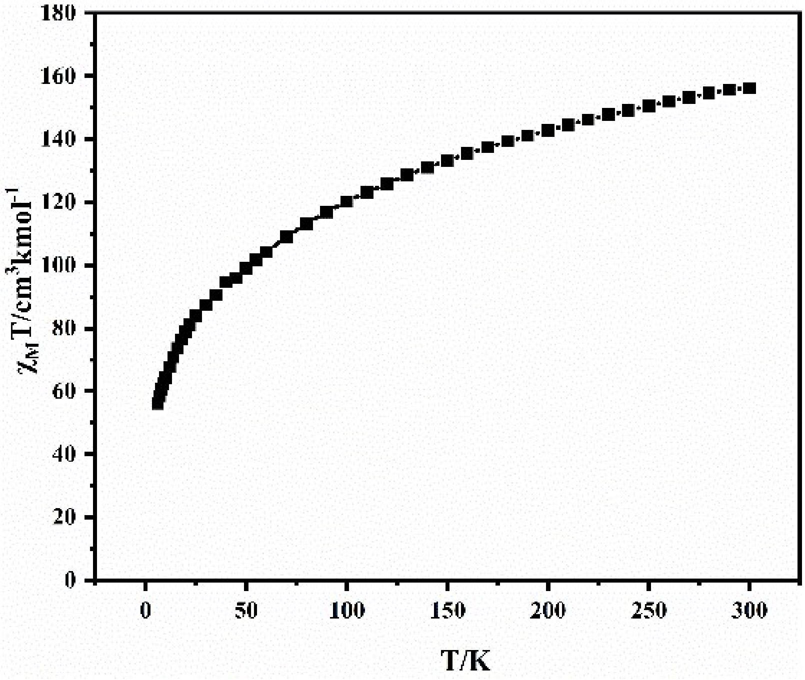

Fig. S10. A Plot of χ_MT vs T for **1**.

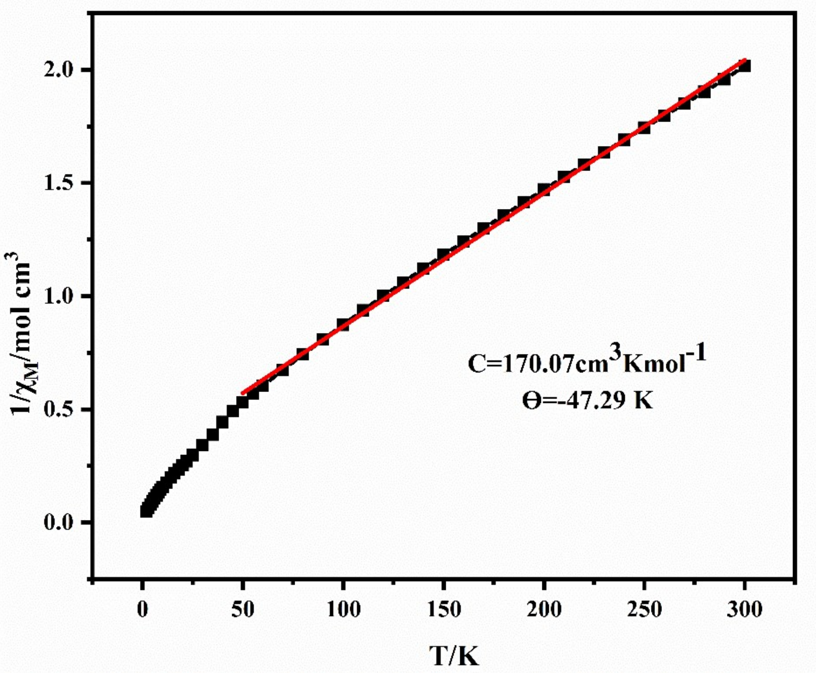

Fig. S11. The χ_m^{-1}-T plot for **1.**

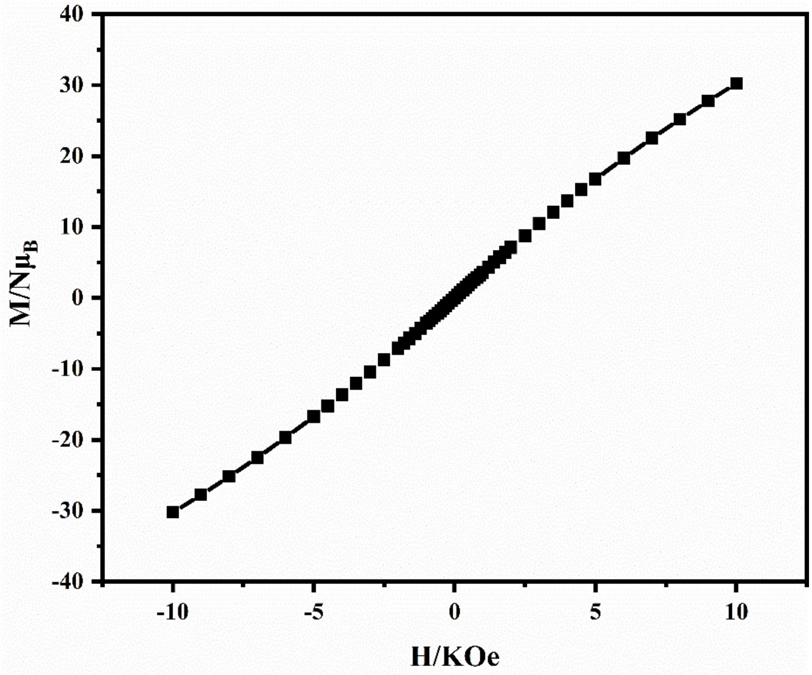

Fig. S12. Field dependence of the magnetization at 2.0 K of **1**.

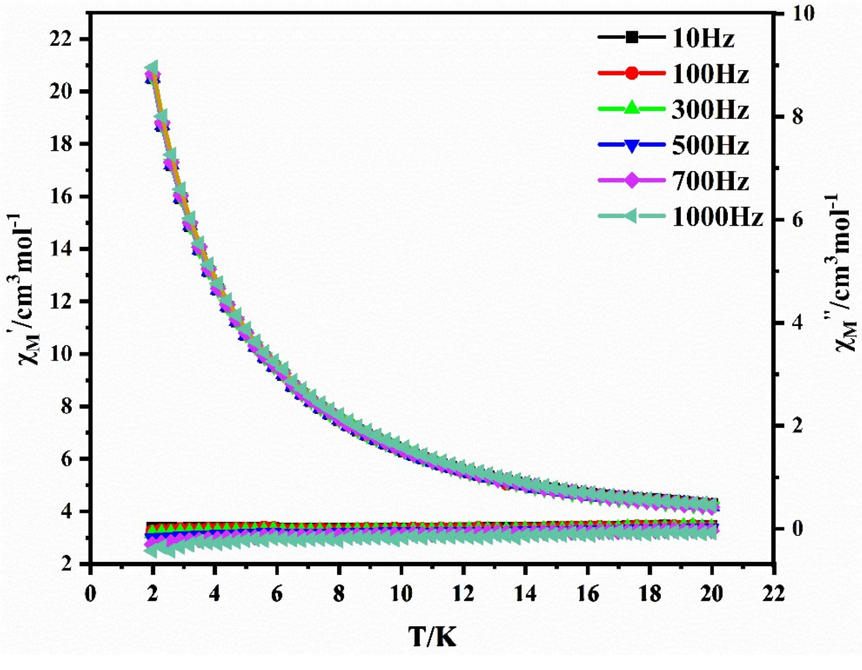

Fig. S13. Out-of-phase ac χ'_M and χ''_M *vs* T at the indicated frequencies for **1**.

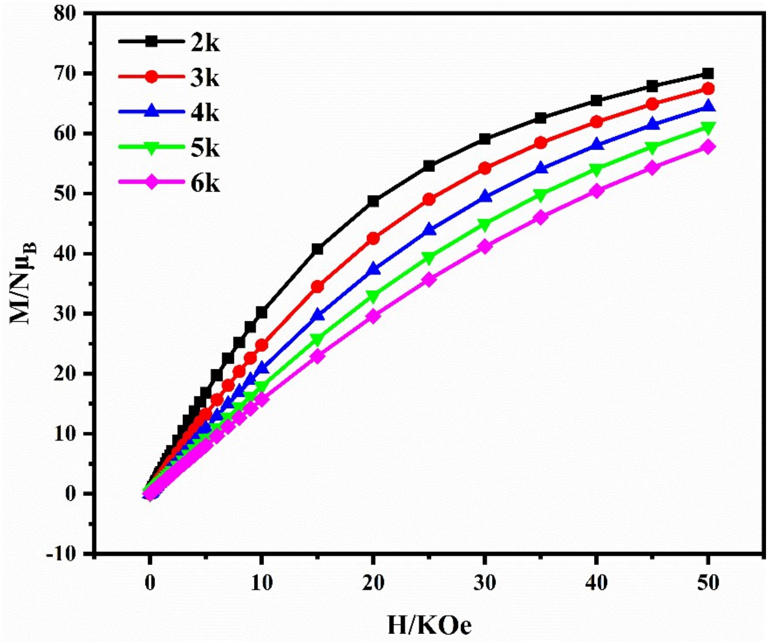

Fig. S14. The plot of *M-H* for **1** in the field rang of 0-50 kOe at 2-6 K.

References

(1) O. V.Dolomanov, L. J.Bourhis, R. J.Gildea,J. A. K.Howard, H.Puschmann, *J . Appl. Crystallogr.*, **2009**, *42*, 339-341.

(2) G. M. Sheldrick, *Acta. Crystallogr A.*, **2008**, *A64*, 112-122.

(3) G. M.Sheldrick, *Acta. Crystallogr C.*, **2015**, *C71*, 3−8.

(4) A. L. Spek, *J. Appl. Cryst.* **2003**, *36*, 7-11.

(5) A.L.Spek, *Acta Cryst.* **2009**, *D65*, 148-155.

(6) A.L.Spek, *Inorg. Chim. Acta* **2018**, *470*, 232-237.

(7) A.L.Spek, *Acta Cryst.* **2020**, *E76*, 1-11.